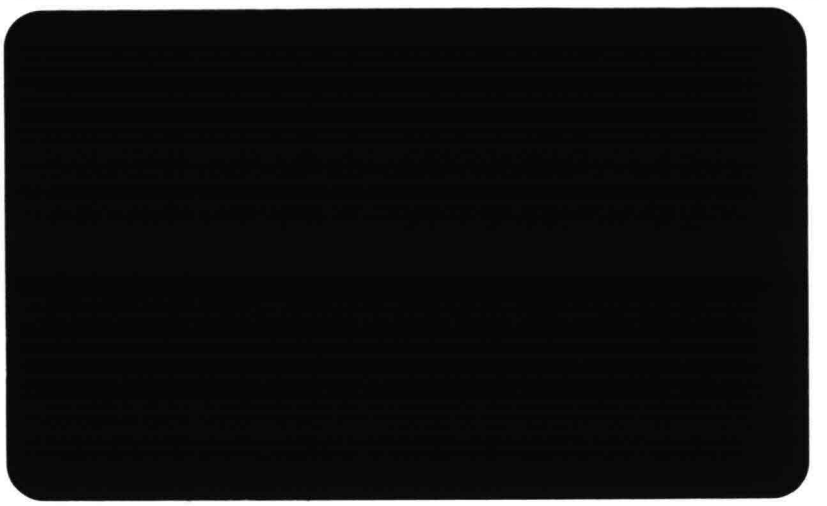

TU Delft
Technische Universiteit Delft

Faculteit der Civiele Techniek
Vakgroep Waterbouwkunde

A model for breach growth in a sand-dike and its prediction for the Zwin 94 experiment

Paul J. Visser

Report no. 12-94

Commissioned by Rijkswaterstaat, Dienst Weg- en Waterbouwkunde

Hydraulic and Geotechnical Engineering Division
Faculty of Civil Engineering
Delft University of Technology
October 1994

Contents

Abstract

A mathematical model for breach growth in sand-dikes and dunes is described. The model is based on the five-step breach erosion process as observed in several laboratory experiments and the Zwin 89 field experiment. A simplified Galappatti (1983) pick up mechanism for sand from the bed is combined with Bagnold's (1963) modified (Visser, 1988) energetics-based sand transport conception to describe the breach erosion. The test of the model to the data of the Zwin 89 experiment shows good agreement. Finally, a prediction for the growth of the breach width in the Zwin 94 experiment is given.

1 Introduction

The Technical Advisory Committee on Water Defences (TAW) in The Netherlands has decided to develop a probabilistic design method for dikes and dunes (hereafter both termed dikes). This method will hold a procedure for the design and control of dikes based on a risk-norm (risk of inundation) instead of on a chance-norm (chance of exceeding a certain water level) as in the present method. A risk-norm means that the inundation chance is combined with the consequences of flooding (deaths, loss of property and revenues, repair costs, etc.). To determine the consequences of an inundation, it is necessary to predict both the rate and speed of polder flooding, which are especially governed by the flow rate through the breach in the dike. This discharge rate largely depends on the process of breach growth.

The final aim of the investigation is a mathematical model, that describes the breach growth and the discharge rate through the breach in case of a dike-burst, as function of the parameters involved. These parameters are:

- cross-section of the dike (height, width, angles of the slopes);
- structure of the dike (dike material, revetments, foundation);
- hydraulic conditions (water level against the dike, wave load).

A first version of the model (Visser, 1988) was especially developed for the huge (about 75 m high) sand-dike of a proposed pumped-storage plant in The Netherlands. Visser et al. (1990) extended the model and confronted it with the data of the Zwin 89 field experiment, yielding reasonable agreement for the first three phases (see chapter 3) of the breach erosion process. This model version was not yet applicable to the last two phases of that process. If applied, it would fairly overestimate the breach growth in these phases.

This report includes (in chapters 2, 3 and 4) a new version of the model, as presented at the 24th International Conference on Coastal Engineering, 23-28 October 1994, Kobe, Japan, (see Visser, 1994b). Its improvements with respect to the previous version are:

- inclusion of a description of the breach erosion in phase IV;
- an improved description of the erosion mechanism in phases I, II and III; these improvements refer to both the physics and the mathematical treatment.

As yet phase V of the breach erosion process has not been included in the model. This phase is important since it yields the final breach dimensions. The present model version (which as yet is restricted to sand-dikes) is tested to the data of the Zwin 89 experiment (chapter 5). Chapter 6 gives a prediction for the increase of the breach width in the Zwin 94 experiment (which is performed 6 and 7 October 1994); this has been done for Rijkswaterstaat, Dienst Weg- en Waterbouwkunde.

2 Entrainment and transport of sediment

Fig. 1 shows a typical cross-section of a sand-dike along the breach axis in the initial phase of the breach erosion process. A coordinate system (x,z) is adopted with coordinate x along the inner slope ($x = 0$ at the top of the dike) and coordinate z normal to the slope. H_w is the water level at sea, Z_T is the height of the top of the dike in the breach (both H_w and Z_T are measured above the base of the dike), and the angles of the outer and inner slope are α and β, respectively.

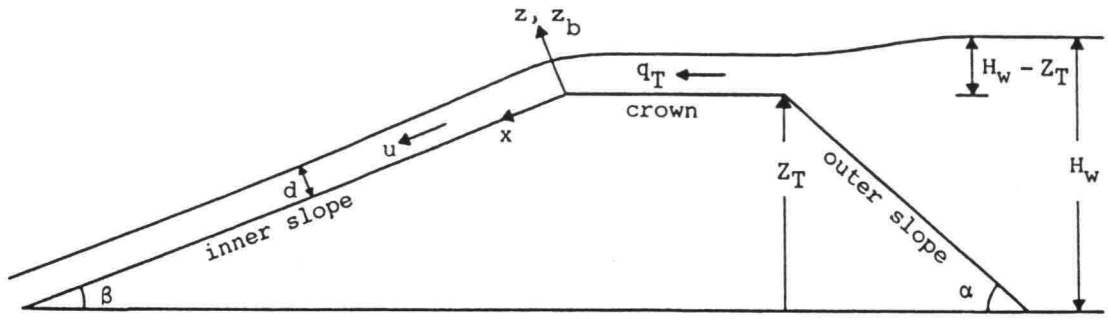

Fig. 1. Typical cross-section of a sand-dike along the breach axis.

The entrainment of sand from the horizontal crown of the dike is very small compared with the pick up from the inner slope, see Steetzel and Visser (1992) and Visser (1994a). The pick up of sand starts at the upstream end of the inner slope ($x = 0$).
For large values of $u_\star/w_s = C_f^{1/2}u/w_s$ (is of order 10 in the present situation, so suspended load transport will dominate bed load transport), the entrainment and subsequent transport of suspended sediment along the inner slope can be approximated according to Galappatti (1983, see also Galappatti and Vreugdenhil, 1985) by:

$$s(x) \approx \frac{x}{l_a} s_s \qquad \text{for} \quad 0 \le x \le l_a \tag{1}$$

in which $s(x)$ is the sediment transport (volumes of particles) per unit width along the slope and l_a is the adaptation length of the suspended load transport:

$$l_a = \frac{ud}{w_s \cos\beta} = \frac{q_T}{w_s \cos\beta} \tag{2}$$

and s_s is the capacity of the suspended load transport:

$$s_s = \frac{0.01}{(w_s/u)(\cos\beta)^2} \frac{C_f u^3}{g\Delta} \quad [\mathrm{m}^2/\mathrm{s}] \tag{3}$$

where u is the depth-averaged flow velocity, d is the water depth (see Fig. 1), w_s is the fall velocity of sand in water, q_T is the discharge flow rate over the dike-top per unit width, C_f is the bed friction coefficient ($C_f = g/C^2$, with C is the Chézy coefficient), $\Delta = (\rho_s - \rho)/\rho$, ρ_s is the mass density of sand, ρ is the water mass density and g is the acceleration of gravity, see Visser (1988). Equation (3) rests on a modified (Visser, 1988) Bagnold (1963) energetics-based sand transport conception for suspended sediment load. The efficiency factor 0.01 is according to Bagnold (1966).

Equation (3) emerges as the best formula out of 15 sand transport formulae in a test with the flume data of Steetzel and Visser (1992) and the data of the Zwin 89 experiment, with Van Rijn's (1984a, 1984b) formulation finishing at the second place, see Visser (1994a). Most of the other formulae overestimate the measured sediment transport rates significantly, also those formulae which were developed for sand-water mixture flows at high shear stress (for instance Wilson, 1987) and for sediment transport on steep slopes (for instance Rickenmann, 1991). For the moment this conclusion (and the choice for (3)) holds for the first three phases of the breaching process when the flow is supercritical.

3 Breach erosion process

3.1 Discharge rate

The water discharge rate q_T per unit breach width is described by a weir formula:

$$q_T = m(2/3)^{3/2} g^{1/2} (H_w - Z_T)^{3/2} \tag{4}$$

where m is the discharge coefficient (≈ 1.0). Equation (4) holds as long as the flow in the breach is not affected by the downstream water level, i.e. for phases I through IV (see paragraph 3.2).

3.2 Erosion of inner slope

The equation for the erosion of the inner slope is:

$$(1 - p)\frac{\partial z_b}{\partial t} + \frac{\partial s}{\partial x} = 0 \tag{5}$$

where p is the bed porosity, z_b is the position of the inner slope in z-direction (z is the coordinate normal to the inner slope, see Fig. 1). Substitution of (1), (2) and (3) into (5) yields:

$$\left|\frac{\partial z_b}{\partial t}\right| = \frac{0.01\, C_f}{(1 - p) g \Delta} \left|\frac{\partial}{\partial x}\left[\frac{x u^4}{q_T \cos\beta}\right]\right| \tag{6}$$

in which it has been assumed that the friction coefficient C_f is constant.

If q_T is constant (that is if $H_w - Z_T$ = constant , see equation (4)) and assuming $\cos\beta \approx 1$, it follows from (6) that:

$$\frac{\partial}{\partial x}\left|\frac{\partial z_b}{\partial t}\right| > 0 \qquad \text{for} \quad 0 < x < l_n \tag{7}$$

since the flow velocity u increases in positive x-direction for $0 < x < l_n$. So the erosion of

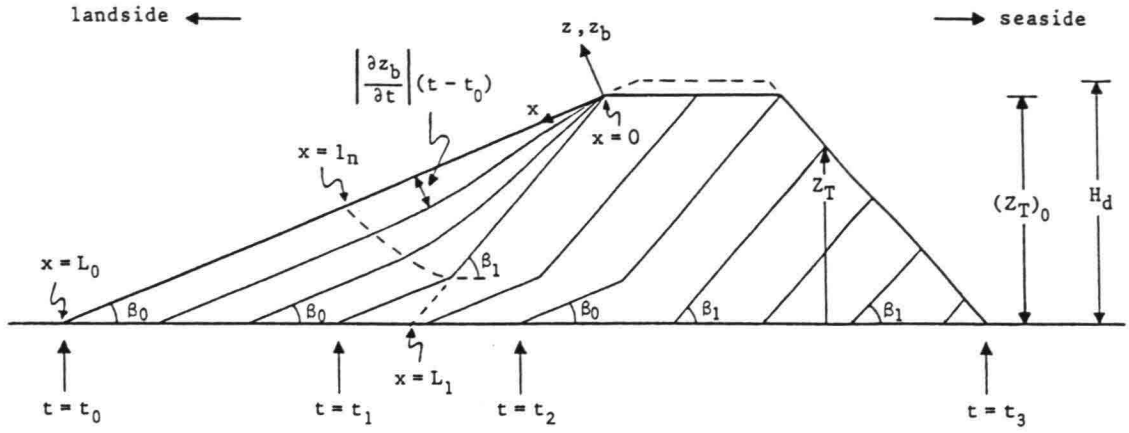

Fig. 2. Erosion of inner slope.

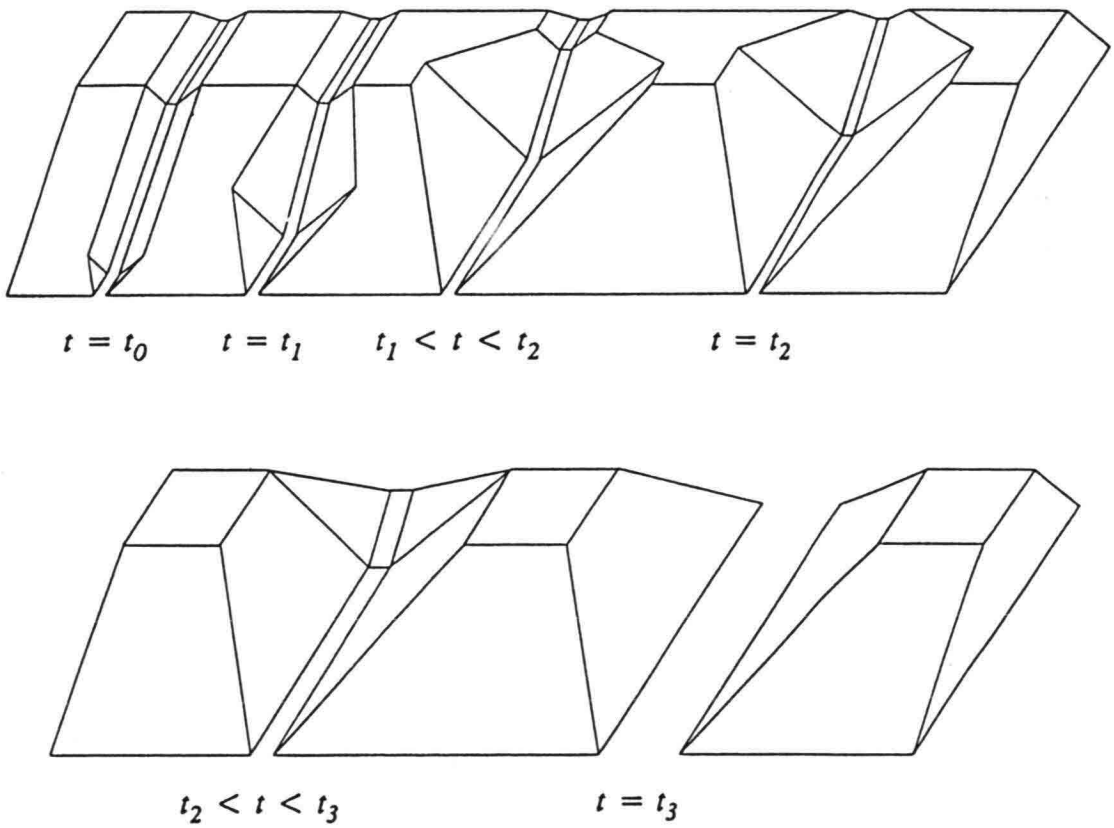

Fig. 3. Process of breach erosion (first phases).

the inner slope increases along the slope and the inner slope becomes steeper in x-direction and in time (see Fig. 2).

For $x = l_n$ the flow velocity u approaches the normal value for uniform flows:

$$u_n = \frac{(g d_n \sin\beta)^{1/2}}{C_f^{1/2}} = \frac{(g q_T \sin\beta)^{1/3}}{C_f^{1/3}} \tag{8}$$

Substitution of (1), (2), (3) and (8) into (5) gives:

$$\frac{\partial z_b}{\partial t} = - \frac{0.01}{(1-p)\Delta} \frac{\partial}{\partial x}\left(x u_n \tan\beta\right) \qquad \text{for} \quad l_n \le x \le l_a \tag{9}$$

If q_T and β are constant then u_n is constant and (9) becomes:

$$\frac{\mathrm{d}z_b}{\mathrm{d}t} = - \frac{0.01}{(1-p)\Delta} u_n \tan\beta \qquad \text{for} \quad l_n \le x \le l_a \tag{10}$$

This means that:

$$\frac{\partial}{\partial x}\left|\frac{\mathrm{d}z_b}{\mathrm{d}t}\right| = 0 \qquad \text{for} \quad l_n \le x \le l_a \tag{11}$$

i.e. the erosion of the inner slope is constant for these values of x, see Fig. 2.

The inner slope becomes steeper for $0 \le x < l_n$. However, the slope angle will not exceed a limit β_1, say $\beta_1 \approx \phi$ (ϕ is angle of repose). If this limit has been achieved on the entire stretch $0 \le x \le l_n$ (on $t = t_1$), then the erosion rate becomes constant for $0 \le x < l_n$, as indicated by the lines for $t \ge t_1$ in Fig. 2.

So, if the breaching process starts at $t = t_0$ with the flow of water through a small initial channel in the crown and the inner slope of the dike, then the following subsequent phases can be distinguished in this process (see Figures 2 and 3):

I. Steepening of the inclination angle (β) of (the initial channel in) the inner slope from an initial value β_0 up to a critical value β_1 at $t = t_1$ (see Fig. 2).

II. Continuation of the erosion of the inner slope, yielding a decrease of the length of the

dike-top in the breach for $t_1 < t < t_2$; the inner slope angle remains (in this line of thoughts) at its critical value β_1.

III. Lowering of the top of the dike in the breach and a subsequent increase of the breach width for $t_2 \leq t \leq t_3$.

IV. After the complete wash-out of the dike in the breach, continuation of the breach growth in vertical (scour hole) and in horizontal direction for $t_3 < t \leq t_4$. At t_4 the flow through the breach is critical, i.e. changes from supercritical ($Fr > 1$ for $t < t_4$) into subcritical ($Fr < 1$ for $t > t_4$).

V. Continuation of the breach growth in horizontal direction for $t_4 < t < t_5$. At t_5 the flow velocities in the breach become so small (incipient motion) that the breach erosion stops.

In phase I the width of the breach remains at its initial small value. At $t = t_1$ the breach width starts to increase at the downstream side of the dike-top (so in phase II the breach eats its way into the dike, see Fig. 3). At $t = t_2$ the width of the breach at the upstream side of the dike-top also starts to grow. In a first estimation the breach width growths directly proportional to the breach depth, see Visser (1988). The discharge rate through the breach starts to increase at $t = t_2$. In the period $t_3 < t < t_4$ the scour hole gets its maximum depth. Phases IV and V are the most important stages, since in the period $t_3 < t < t_5$ most of the water is discharged through the breach and the ultimate dimensions of the breach are determined.

4 Model description

4.1 Steepening of the inner slope (phase I)

The erosion of the inner slope is described by (5) with (1), (2), (3) and an equation for the flow velocity. The flow velocity u follows from (4) and an equation for the non-uniform flow depth along the stretch $0 < x < l_n$. Consequently a numerical method is necessary to describe the development of the entire inner slope for $t_0 < t < t_1$.

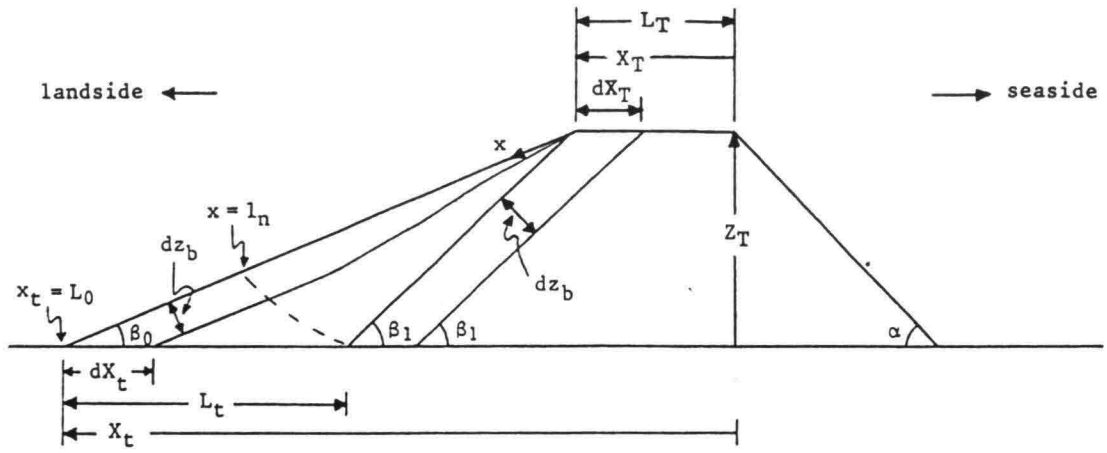

Fig. 4. Horizontal displacements dX_t and dX_T due to erosion dz_b of inner slope.

An analytical solution for phase I is possible along the stretch $l_n \le x \le l_a$, where equation (10) describes the erosion rate dz_b/dt. The horizontal displacement dX_t of the toe of the inner slope can simply be expressed in dz_b (see Fig. 4):

$$dX_t = \frac{1}{\sin\beta_0} dz_b \tag{12}$$

Substitution of (4), (8), (10), $\beta = \beta_0$ and $Z_T = (Z_T)_0$ into (12) yields for $t_0 \le t \le t_1$:

$$\frac{dX_t}{dt} = -k_0 \sqrt{H_w - (Z_T)_0} \qquad \text{for} \quad l_n \le x_t \le l_a \tag{13}$$

where x_t is the x-coordinate of the toe of the inner slope (see Fig. 4) and:

$$k_0 = \frac{0.0082}{(1-p)\Delta} (m/C_f)^{1/3} g^{1/2} \frac{(\sin\beta_0)^{1/3}}{\cos\beta_0} \tag{14}$$

If $l_n = L_1$ at $t = t_1$ then:

$$\int_{t_0}^{t_1} dX_t = -L_t \tag{15}$$

Substitution of (13) into (15) finally yields:

$$t_1 - t_0 = \frac{L_t}{k_0 \sqrt{H_w - (Z_c)_0}} \tag{16}$$

If $L_1 > l_n(t_1)$ then ξL_t as defined in Fig. 5 should replace L_t in equation (16).

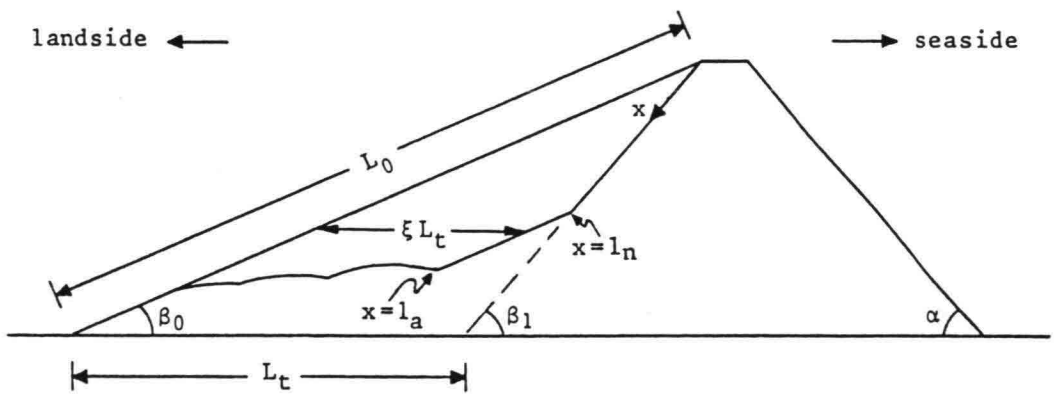

Fig. 5. Erosion of inner slope for relatively high dikes.

4.2 Decrease of crown length (phase II)

At $t = t_1$ the steepness of the inner slope is at its critical value (angle β_1). From now on the rate of erosion is constant along the entire stretch $0 \leq x \leq l_a$, see Fig. 2. Consequently the erosion of the inner slope for $t_1 < t < t_2$ is entirely determined by the erosion at the toe of the slope ($x = L_1$) as long as $L_1 < l_a$:

$$-L_1(1-p)\frac{dz_b}{dt} = s(L_1) = \frac{L_1}{l_a}s_s(L_1) \tag{17}$$

Generally $L_1 > l_n$ (see Visser, 1994a), so $u(L_1) = u_n$. The substitution of (2), (3) and (8) with $\beta = \beta_1$ into (17) yields in agreement with (10):

$$\frac{dz_b}{dt} = -\frac{0.01}{(1-p)\Delta}u_n \tan\beta_1 \qquad \text{for} \quad 0 \leq x \leq L_1 \tag{18}$$

Fig. 4 shows that in the breach the length of the dike-top (original value L_T) decreases for $t_1 < t < t_2$ due to the erosion of the inner slope. The relation between the decrease of the length of the dike-top (dX_T) and the erosion of the inner slope (dz_b) is:

$$dX_T = \frac{1}{\sin\beta_1}dz_b \tag{19}$$

Substitution of (4) with $Z_T = (Z_T)_0$, (8) with $\beta = \beta_1$ and (18) into (19) gives:

$$\frac{dX_T}{dt} = -k_1\sqrt{H_w - (Z_T)_0} \qquad \text{for} \quad t_1 \leq t \leq t_2 \tag{20}$$

with:

$$k_1 = \frac{0.0082}{(1-p)\Delta}(m/C_f)^{1/3}g^{1/2}\frac{(\sin\beta_1)^{1/3}}{\cos\beta_1} \tag{21}$$

Integration of (20) gives:

$$t_2 - t_1 = \frac{L_T}{k_1 \sqrt{H_w - (Z_T)_0}} \tag{22}$$

Visser (1988) argues that due to the increase of the breach width an extra amount of sand falls into the flow, slowing down the breach erosion in vertical direction (with a factor f compared with a 2-D situation; to a lesser extent this applies also to phase I). The factor f will vary from phase to phase. Assuming f to be constant in each phase, equation (22) becomes for the 3-D situation:

$$t_2 - t_1 = \frac{L_T}{f_1 k_1 \sqrt{H_w - (Z_T)_0}} \tag{23}$$

4.3 Decrease of crown level (phase III)

At $t = t_2$ the top of the dike in the breach starts to drop. The relation between the fall dZ_T of the top and the rate of erosion dz_b of the inner slope follows from a simple geometrical consideration (see Fig. 6):

$$dZ_T = \frac{\sin\alpha}{\sin(\alpha + \beta_1)} dz_b \tag{24}$$

Substitution of (4), (8) with $\beta = \beta_1$ and (18) into (24) yields:

$$\frac{dZ_T}{dt} = - k_2 \sqrt{H_w - Z_T} \quad \text{for} \quad t_2 \leq t \leq t_3 \tag{25}$$

where:

$$k_2 = \frac{\sin\alpha \sin\beta_1}{\sin(\alpha + \beta_1)} k_1 \tag{26}$$

At $t = t_2$ the width of the breach at the upstream end of the dike-top starts to increase. Visser (1988) argues that the breach width (so also the depth-averaged breach width B) increases linearly with the growth of the breach depth $H_d - Z_T$:

$$\frac{dB}{dt} = r\,\frac{d(H_d - Z_T)}{dt} \qquad \text{for} \quad t_2 \le t \le t_3 \tag{27}$$

where r is a coefficient with a theoretical value (for sand-dikes) of about 2.2 for the depth-averaged breach width and about 3.8 for the breach width at the top of the dike.
Due to the increase of the breach width an extra amount of sand falls into the flow, slowing down the breach erosion in vertical direction (with a factor f_2 in this stage, see paragraph 4.2). Hence equation (25) becomes:

$$\frac{dZ_T}{dt} = -f_2 k_2 \sqrt{H_w - Z_T} \qquad \text{for} \quad t_2 \le t \le t_3 \tag{28}$$

in which the factor f_2 (see Visser, 1988) is:

$$f_2 = \frac{B + 2q_T/u}{2B} \tag{29}$$

Integration of (28) gives with $Z_T = 0$ at $t = t_3$:

$$Z_T(t) = H_w - \left[\frac{f_2 k_2}{2}(t - t_3) + \sqrt{H_w}\right]^2 \qquad \text{for} \quad t_2 \le t \le t_3 \tag{30}$$

Substitution of $Z_T = (Z_T)_0$ at $t = t_2$ into (30) gives:

$$t_3 - t_2 = \frac{2}{f_2 k_2}\left[\sqrt{H_w} - \sqrt{H_w - (Z_T)_0}\right] \tag{31}$$

If the depth of the initial breach ($H_d - (Z_T)_0$, see Fig. 2) is small compared with the dike-height H_d (so also small compared with H_w), then (31) reduces to:

$$t_3 - t_2 = \frac{2}{f_2 k_2}\sqrt{H_w} \tag{32}$$

4.4 Continuation of breach growth (phase IV)

Locally the dike has been completely washed out ($Z_T = 0$) at $t = t_3$ and the breach continues to grow in both vertical (scour hole: $Z_T < 0$) and horizontal direction for $t > t_3$. The equation for the discharge rate q_T per unit of breach width is for $t_3 \le t \le t_4$:

$$q_T = m(2/3)^{3/2} g^{1/2} (H_w)^{3/2} \tag{33}$$

The scour hole has an upstream slope (β_3, bed elevation decreasing in flow direction: β_3 is not equal to β_1) and a downstream slope (bed elevation increasing in flow direction). It is assumed that the breach growth in phase IV is determined by the erosion of the upstream

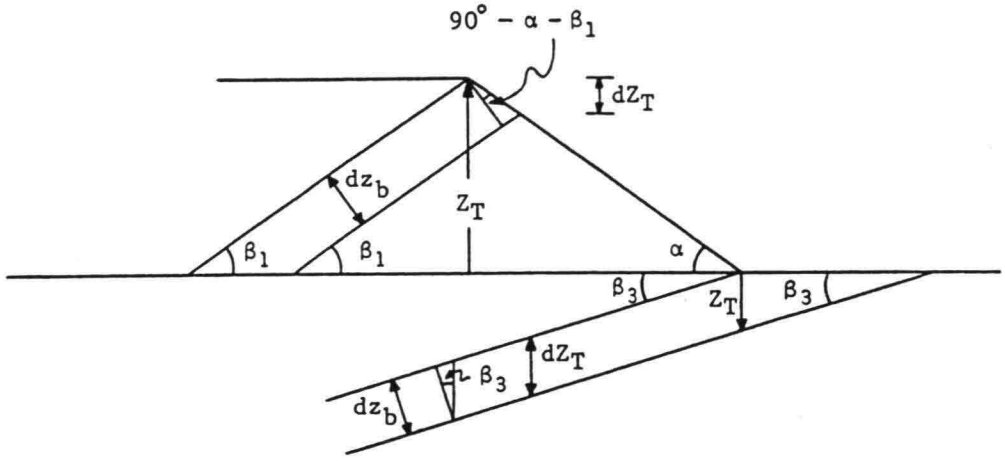

Fig. 6. Relation between dZ_T and dz_b in phases III and IV.

slope of the scour hole. Then equation (10) describes also the erosion in vertical direction in phase IV:

$$\frac{dz_b}{dt} = -\frac{0.01}{(1-p)\Delta} u_n \tan\beta_3 \qquad \text{for} \quad l_n \le x \le l_a \tag{34}$$

The relation between the increase of the depth of the scour hole dZ_T and the rate of erosion dz_b of the upstream slope of the scour hole follows from a simple geometrical consideration (see Fig. 6):

$$dZ_T = \frac{1}{\cos\beta_3} dz_b \tag{35}$$

Substitution of (8) with $\beta = \beta_3$, (33) and (34) into (35) and including a factor f yields:

$$\frac{dZ_T}{dt} = -f_3 k_3 \sqrt{H_w} \qquad \text{for} \quad t_3 \le t \le t_4 \tag{36}$$

with:

$$k_3 = \frac{0.0082}{(1-p)\Delta} (m/C_f)^{1/3} g^{1/2} \frac{(\sin\beta_3)^{4/3}}{(\cos\beta_3)^2} \tag{37}$$

Integration of (36) gives with $Z_T = 0$ at $t = t_3$:

$$Z_T(t) = -f_3 k_3 \sqrt{H_w} (t - t_3) \qquad \text{for} \quad t_3 \le t \le t_4 \tag{38}$$

It is assumed that (27) holds also in phase IV; then substituting (38) into (27) gives the increase of the breach width for $t_3 \le t \le t_4$. For the initial stage of phase IV this assumption seems reasonable. It is, however, rather obvious that the validity of (38), and consequently also (27), has its limits, otherwise large breach depths are necessary to explain the existence of relatively wide breaches.
One of the main aims of the Zwin 94 experiment has been to solve this uncertainty about the growth of the scour hole and its relation with the increase of the breach width in phase IV.

5 Comparison with data of Zwin 89 experiment

The present breach erosion model is tested to the data of the Zwin 89 experiment. This large scale experiment was performed in the Zwin Channel (a tidal inlet in the south-western part of The Netherlands) in December 1989, see Visser et al. (1990).

The dimensions of the sand-dike in the Zwin 89 experiment have been: $H_d = 2.2\,\text{m}$ (above the bottom of the Zwin channel, which was at about NAP[1] + 0.3 m), $L_T \approx 7.5\,\text{m}$, $\beta_0 = 18.4°$ (inner slope 1 : 3) and $\alpha = 39°$ (outer slope 1 : 1.25), see Fig. 7. The sand-dike (with a length of approximately 60 m) was constructed, exclusively for the experiment, with local sand $D_{50} \approx 0.22\,\text{mm}$. A small pilot channel (initial breach), about 9 m long, about 1 m wide and with a depth $H_d - (Z_c)_0 \approx 0.35\,\text{m}$ was made in the dike-top to ensure breaching near the middle of the Zwin Channel.

The breaching process was both video-taped and photographed. Levelling-staffs in the crown of the dike provided the proper length-scale for the readings from the video-tape and the photographs. The main result of these readings, i.e. the development of the 'depth-averaged' breach width $B(t)$ at the downstream end of the crown of the dike, is shown in Fig. 8. These data differ slightly from those in Visser et al. (1990), where breach width $B(t)$ was given as averaged (both along the breach length and in depth) value of observed breach width.

The comparison of the model prediction with the data of the Zwin 89 experiment has been done with the following values for the different parameters: $p = 0.4$, $\Delta = 1.65$, $m = 1.0$, $f_1 = f_2 = f_3 = 0.6$ (estimated with equation (29)), $C_f = 0.015$, $\beta_1 = 32°$ (see Visser et al., 1990) and $r = 2.2$ (for depth-averaged breach width). For β_3 the value found by Delft Hydraulics (1972) for scour holes has been adopted: $\beta_3 \approx 12°$ ($\tan\beta_3 \approx 0.2$). This is a crude assumption since there exists no universal value for this angle.

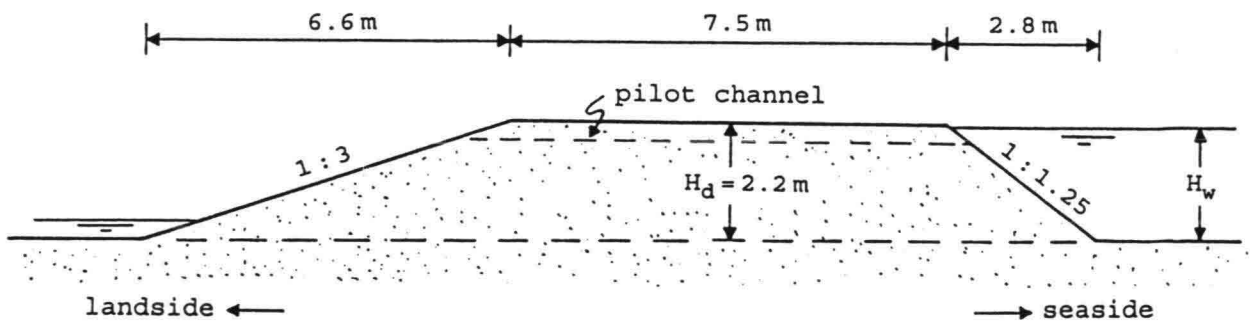

Fig. 7. Cross-section of sand-dike in Zwin 89 experiment.

[1] Reference level in the Netherlands, at about mean sea level

Setting $t_0 = 0$, substitution of these values into (16) with (14) yields $t_1 = 1.5$ min (in this phase : $H_w - (Z_T)_0 \approx 0.13$ m), substitution into (23) with (21) gives $t_2 - t_1 = 5.0$ min (in phase II: $H_w - (Z_T)_0 \approx 0.17$ m), so $t_2 = 6.5$ min, and into (31) with (26) gives $t_3 - t_2 = 1.2$ min (in phase III: $H_w \approx 2.1$ m), so $t_3 = 7.7$ min. The increase of the breach width $B(t)$ is given by (27) with (28) in phase III and by (27) with (36) in phase IV. The results of the model prediction for $B(t)$ for the Zwin 89 experiment are shown in Fig. 8. The kink for $t = t_3$ is due to keeping β at β_1 for $t_2 \leq t \leq t_3$, while in reality β will decrease from β_1 to β_3 in this phase.

The experimental data (flow velocities and water levels measured upstream and downstream form the breach) indicate that $t_4 \approx 20$ min, see Visser et al. (1990). Hence Fig. 8 shows the development of the breach width $B(t)$ in phases I through IV.

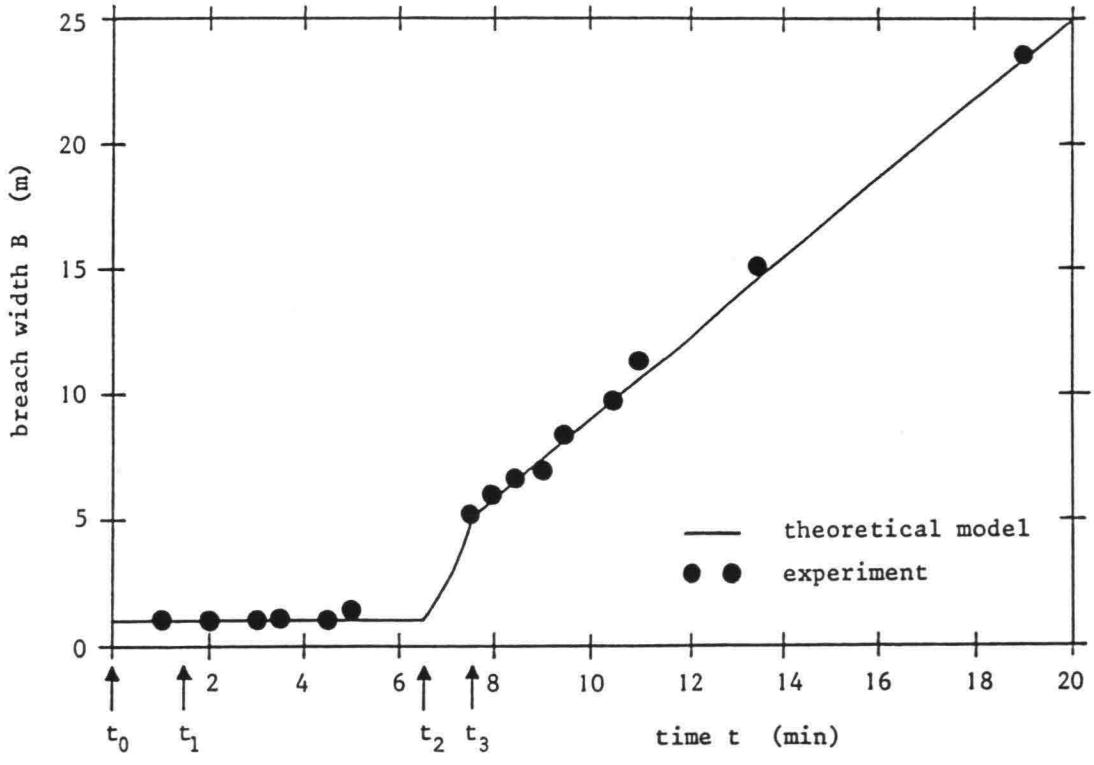

Fig. 8. Comparison of measured (Zwin 89 experiment) and computed breach width $B(t)$ at the upstream end of the dike-top.

6 Prediction increase breach width in Zwin 94 experiment

Finally a prediction[2] for the increase of the breach width $B(t)$ in the Zwin 94 experiment is given. As described in the previous chapters, the present model version can be applied for $t_0 \leq t \leq t_4$; as yet it cannot predict the breach erosion process in the final phase (phase V, $t_4 < t \leq t_5$). A prediction for the breach growth in phase V in the Zwin 94 field experiment can (only) be given using and extrapolating the data of the Zwin 89 experiment. The photos of the Zwin 89 experiment indicate that at $t = 30$ min the breach width was $B \approx 35$ m. The extrapolation for $B(t)$ in the Zwin 89 experiment using this additional measuring point is given in Fig. 9: a final, maximum breach width $B_{max} \approx 40$ m at $t \approx 50$ min to 60 min.

The Zwin 94 experiment is performed (on 6 and 7 October 1994) at the same location as the Zwin 89 experiment. The dimensions of the sand-dike in the Zwin 94 experiment are: length of about 70 m, $H_d = 3.0$ m, $L_T = 8.0$ m, $\beta_0 = 18.4°$ and $\alpha = 39°$. The sand-dike is built with local sand $D_{50} \approx 0.22$ mm. The experiment is done at a high water level $H_w \approx 2.4$ m (above the bottom of the Zwin Channel, which is still at about NAP + 0.3 m). A small pilot channel, about 12 m long, with a depth $H_d - (Z_T)_0 \approx 0.80$ m and with a depth-averaged width of about 2 m is made in the dike-top to ensure breaching near the middle of the Zwin Channel.

The model prediction is done with the same values for the different parameters as used before: $p = 0.4$, $\Delta = 1.65$, $m = 1.0$, $f_1 = f_2 = f_3 = 0.6$, $C_f = 0.015$, $\beta_1 = 32°$, $r = 2.2$ and $\beta_3 \approx 12°$ ($\tan\beta_3 \approx 0.2$). It is assumed that the water level remains at $H_w \approx 2.4$ m, so $H_w - (Z_T)_0 \approx 0.20$ m. Again setting $t_0 = 0$, substitution of these values into (16) with (14) yields $t_1 = 1.5$ min, substitution into (23) with (21) gives $t_2 - t_1 = 5.0$ min ($t_2 = 6.5$ min) and into (31) with (26) gives $t_3 - t_2 = 1.5$ min ($t_3 = 8.0$ min). The increase of the breach width $B(t)$ is described by (27) with (28) in phase III and by (27) with (36) in phase IV. The model prediction for $B(t)$ in the Zwin 94 experiment for $t_0 \leq t \leq t_4$ is shown in Fig. 9 (it is expected that in the Zwin 94 experiment also $t_4 \approx 20$ min).

Theoretically in phase IV dB/dt is proportional to $(H_w)^{1/2}$, see equations (27) and (36). The ratio of the value of $(H_w)^{1/2}$ in the Zwin 89 experiment with that of the Zwin 94 experiment is $(2.4/2.2)^{1/2}$. It is assumed that this ratio also applies to phase V, i.e. that the increment

---

[2] The 'prediction' given in this chapter has been adjusted very slightly after completion of the Zwin 94 experiment. The adjustment has been done since the inclination of the outer slope was about 1 : 1.25 and not the planned 1 : 3 that was applied in the original prediction. In theory the effect of this steeper outer slope is limited to a larger factor k_2 giving a 1.5 min smaller period $t_3 - t_2$ of phase III, see equations (26) and (32).

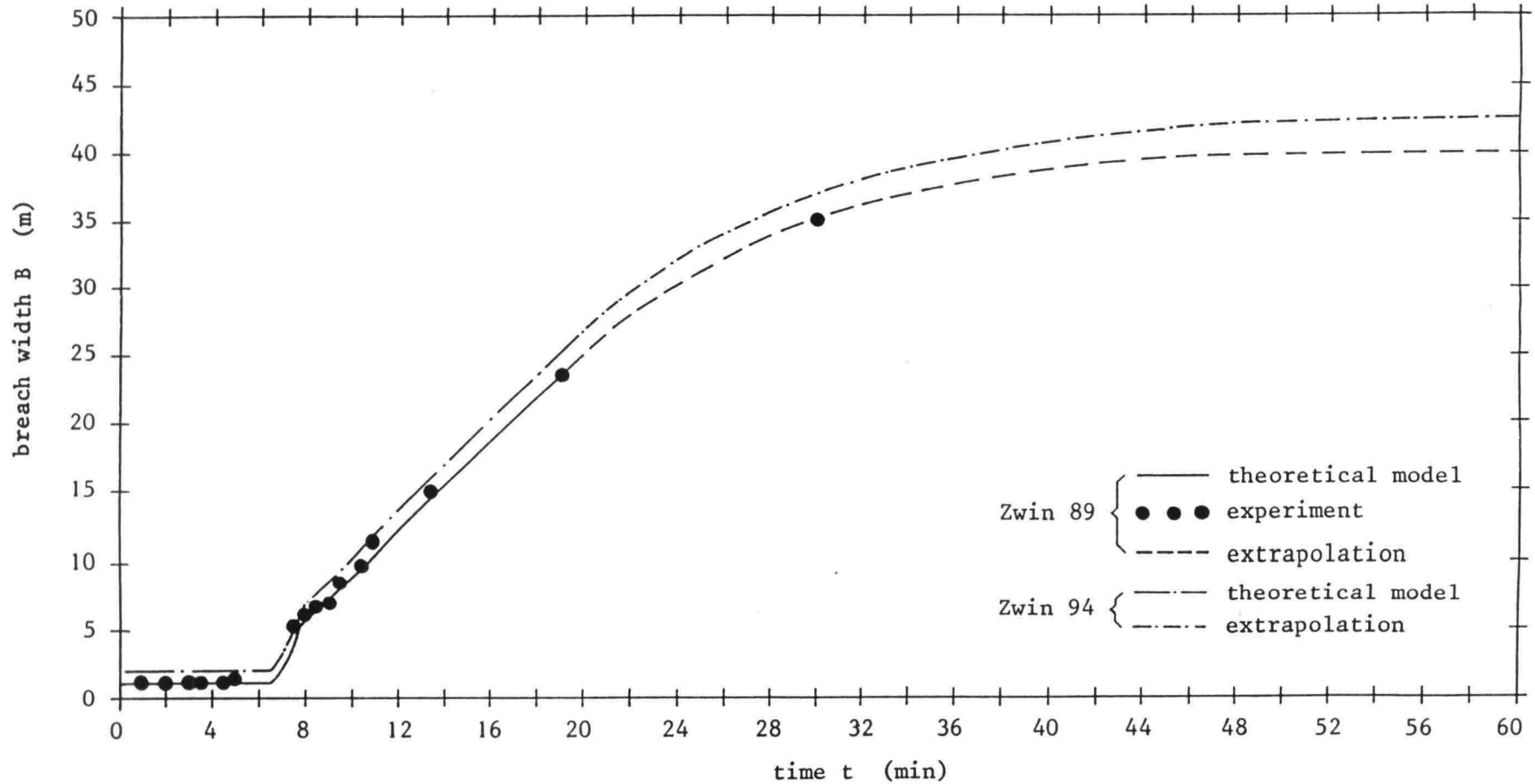

Fig. 9. Extrapolation of growth of breach width B (at the upstream end of the dike-top) in the Zwin 89 experiment and prediction of development of $B(t)$ in the Zwin 94 experiment.

of $B(t)$ in the Zwin 94 experiment in phase V is a factor $(2.4/2.2)^{1/2}$ larger than in the Zwin 89 experiment. The result is shown in Fig. 9, indicating a prediction for the final breach width in the Zwin 94 experiment of $B_{max} \approx 42.5$ m at $t = t_5 \approx 50$ min to 60 min (about equal to the earlier prediction of $B_{max} \approx 42$ m and close to the ultimately in the Zwin 94 experiment observed $B_{max} \approx 44$ m at $t = t_5 \approx 60$ min).

References

Bagnold, R.A., 1963. Mechanics of marine sedimentation. In *'The Sea: Ideas and Observations', 3*, Interscience, New York, USA, pp. 507-528.

Bagnold, R.A., 1966. An approach to the sediment transport problem from general physics. *Geological Survey Professional Paper 422-I*, U.S. Government Printing Office, Washington, USA.

Delft Hydraulics, 1972. Systematic research on two- and three-dimensional scour. *Rep. M648/863* (in Dutch).

Galappatti, R., 1983. A depth-integrated model for suspended transport. *Communications on Hydraulics, Rep. 83-7*, Dept. Civil Eng., Delft Univ. Techn., Delft, The Netherlands.

Galappatti, R. and Vreugdenhil, C.B., 1985. A depth-integrated model for suspended sediment transport. *J. Hydr. Res., 23*, pp. 359-377.

Rickenmann, D., 1991. Hyperconcentrated flow and sediment transport at steep slopes. *J. Hydr. Eng., 117*, pp. 1419-1439.

Van Rijn, L.C., 1984a. Sediment transport. Part I: bed load transport. *J. Hydr. Eng., 110*, pp. 1431-1456.

Van Rijn, L.C., 1984b. Sediment transport. Part II: suspended load transport. *J. Hydr. Eng., 110*, pp. 1613-1641.

Steetzel, H.J. and Visser, P.J., 1992. Profile development of dunes due to overflow. *Proc. 23rd Int. Conf. Coastal Eng.*, Italy, Venice, pp. 2669-2679.

Visser, P.J., 1988. A model for breach growth in a dike-burst. *Proc. 21st Int. Conf. Coastal Eng.*, Malaga, Spain, pp. 1897-1910.

Visser, P.J., 1994a. Application of sediment transport formulae for sand-dike breach erosion. *Communications on Hydraulic and Geotechnical Eng., Rep. no. 94-7*, Dep. Civil Eng., Delft Univ. of Technology, Delft, The Netherlands.

Visser, P.J., 1994b. A model for breach growth in sand-dikes. *Proc. 24th Int. Conf. Coastal Eng.*, Kobe, Japan.

Visser, P.J., Vrijling, J.K. and Verhagen, H.J., 1990. A field experiment on breach growth in sand-dikes. *Proc. 22nd Int. Conf. Coastal Eng.*, Delft, The Netherlands, pp. 2087-2100.

Wilson, K.C., 1987. Analysis of bed-load motion at high shear stress. *J. Hydr. Eng., 113*, pp. 97-103.

Symbols

Symbol	Description	SI-unit
B	depth-averaged breach width (at the downstream end of the dike-top)	[m]
B_{max}	final, maximum value of B	[m]
C	Chézy coefficient	[$m^{0.5}/s$]
C_f	friction coefficient for the bed ($C_f = g/C^2$)	[-]
d	water depth	[m]
D_{50}	median particle diameter	[m]
$f_1 .. f_3$	factors expressing slowing-down effect of erosion in horizontal direction on that in vertical direction in various phases of erosion process	[-]
Fr	Froude number = $u/\sqrt{gd}$	[-]
g	acceleration of gravity	[m/s^2]
H_d	height of dike (above polder surface, in Zwin experiments above bottom Zwin Channel)	[m]
H_w	water level against dike (above polder surface, in Zwin experiments above bottom Zwin Channel)	[m]
$k_0 .. k_3$	breach erosion coefficients, see equations (14), (21), (26), (37)	
L	length inner slope	[m]
l_a	adaptation length of suspended load	[m]
l_n	length along inner slope over which the flow velocity approaches the normal flow velocity	[m]
p	bed porosity	[-]
q	flow discharge	[(m^3/s)/m]
q_T	flow discharge over dike top	[(m^3/s)/m]
r	width-depth ratio of breach	
s_s	capacity of suspended load transport	[(m^3/s)/m]
$s(x)$	sediment transport (volumes of particles) at location x along the inner slope	[(m^3/s)/m]
t	time	[s]
$t_0 .. t_5$	see paragraph 3.2 (pages 5, 6 and 7)	[s]
u	depth-averaged flow velocity	[m/s]
u_n	normal flow velocity (equilibrium value of flow velocity u)	[m/s]
$u_\star$	bed shear velocity	[m/s]
w_s	sediment fall velocity	[m/s]

Symbol	Description	SI-unit
x	coordinate along inner slope ($x = 0$ at the top of the inner slope)	[m]
x_t	x-coordinate of the toe of the inner slope (see Fig. 4)	[m]
X_T	horizontal position of the top of the inner slope with respect to the top of the outer slope (see Fig. 4)	[m]
z	coordinate normal to the inner slope ($z = 0$ at inner slope)	[m]
z_b	position of inner slope in z-direction	[m]
Z_T	height top of dike in breach (above polder surface)	[m]
α	inclination angle of outer slope	[°]
β	inclination angle of inner slope	[°]
Δ	specific density = $(\rho_s - \rho)/\rho$	[-]
ρ	water density	[kg/m^3]
ρ_s	sediment density	[kg/m^3]
ϕ	angle of repose of bed material	[°]